

# Photogrammetric Recording and Modelling of a Valley Floor using RPAS-mounted RGB and TIR Cameras

KONRAD EDER<sup>1</sup>, LUDWIG HOEGNER<sup>1</sup>, WOLFGANG RIEGER<sup>2</sup>, MARIA KAISER<sup>2</sup> & UWE STILLA<sup>1</sup>

*Zusammenfassung: In diesem Beitrag wird ein Projekt zur 3D Modellierung und Auswertung eines Talbodens für die hydrologische Abflusssimulation vorgestellt. Hierfür wurde ein RPAS (Remotely Piloted Aerial System) System eingesetzt, um in aufeinander folgenden Überflügen eine Bildserie jeweils mit einer hochauflösenden photogrammetrischen Kamera und einer thermischen Infrarotkamera aufzuzeichnen. Aus den Bildern der photogrammetrischen Kamera wird ein Digitales Geländemodell erstellt und anschließend ein Ortho imagesaiki gerechnet. Die Bilder der Thermalkamera werden anschließend auf dieses Ortho image koregistriert. Hierdurch ist eine Lokalisierung und Identifikation von im Geländemodell nicht erfassten Oberflächenabflüssen möglich, was zur Verbesserung und Validierung hydrologischer Modelle eingesetzt werden kann.*

*Abstract: This contribution presents a project for 3D modelling and analysis of a valley floor for hydrological simulations. An RPAS (Remotely Piloted Aerial System) is used to mount either a high-resolution photogrammetric camera or a thermal infrared camera in two different, consecutive flights recording an image sequence. The images of the photogrammetric camera are used to generate both a digital terrain model and an orthoimage mosaic. The images of the thermal camera are coregistered to this orthoimage. This allows the localization and identification of surface water flow that is not derivable from the terrain model only. The results can be used to improve and evaluate process based hydrological models.*

## 1 Introduction

Aerial Photogrammetry for generation of digital terrain models and orthoimages is a widely used method. Tie points are automatically detected to connect the images within a set to an image bundle block which is adjusted optimizing the exterior orientation parameters of the images. This procedure is transferable from the visible domain to the thermal infrared domain where the lower geometric resolution reduces the accuracy of the 3D reconstruction. Methods for joint analysis of images from the visible domain and thermal infrared have been introduced to remote sensing (NICHOL & LEE 2004; NICHOL 2005). Most of these methods rely more or less on a flat earth scenario and are invalid for mountainous areas as they do not include digital terrain models. The reconstruction of 3D geometry has been introduced to UAV / RPAS (unmanned aerial vehicle / remotely piloted aerial system) mounted cameras using feature points and onboard inertial measurement units for building reconstruction and cultural heritage (MAYER ET AL. 2012). This work also includes semi-global matching to derive dense point clouds from the whole pixel set of

---

<sup>1</sup> Technische Universität München, Photogrammetry and Remote Sensing, Arcisstrasse 21, D-80333 München, Germany, E-Mail: [Konrad.Eder, Ludwig.Hoegner, stilla]@tum.de

<sup>2</sup> Technische Universität München, Hydrology and River Basin Management, Arcisstrasse 21, D-80333 München, Germany, E-Mail: [Wolfgang.Rieger, Maria.Kaiser]@tum.de

the images instead of only using 3D coordinates for homologous points (HIRSCHMÜLLER 2008). 3D reconstruction from thermal images is investigated for terrestrial (HOEGNER & STILLA 2015) and RPAS mounted (WESTFELD et al. 2015) infrared cameras. The coregistration of the thermal infrared images to the RGB ortho image allows the generation of a thermal orthoimage and the interpolation of thermal infrared intensities for all pixels of RGB orthoimage. The resulting four-channel orthoimage can be used for segmentation and object detection.

In the field of hydrology, the question arises, in which part of a catchment surface runoff is generated and what ways it chooses to concentrate down to the valley ground and catchment outlet. Most of the water follows small runlets down the slopes. These runlets are mainly not included in standard digital terrain models, but are visible in high resolution aerial images. This allows generating a terrain model with a few centimeters grid size. Additionally, many rills show slightly differences in radiometric behavior and can be classified. A relevant percentage of the water is flowing down directly on the surface and these very small flows are mainly invisible in the geometric reconstruction and radiometric classification in the visible domain. In the thermal infrared, the cooling effect of surface water flow shows areas with water present or higher moisture caused by prior water flow. Integrating this information to the RGB image increases and refines the classification accuracy.

To identify the areas of surface runoff generation in a catchment and to quantify the amount of generated surface runoff, physically based hydrological models are used in hydrology. In this context, a suitable method is the Water Balance Simulation Model WaSiM (SCHULLA 1997; 2015), which has been extended in a way that the runoff concentration of surface flow can be determined by a cinematic wave approach (WINTER 2013). This contribution deals with the question how high-resolution aerial images and thermal infrared pictures can help to validate the predicted flow paths of WaSiM in the Sachenbach catchment.

## 2 Methodology

The integration of the thermal image information into the RGB orthoimage and the joint usage for hydrological surveys is split into four parts: In part one, the RGB images are combined into a bundle block. Part two uses detected feature points visible in both the RGB orthoimage and the thermal infrared images to overlay the infrared images to the orthoimage. Part three is a segmentation of possible water flow areas on the slopes and meadows. Part four is about the integration into hydrological modelling.

### 2.1 Ortho Image Generation

It is assumed that all images are taken with an end lap of at least 60% and a side lap of around 40%. The recording positions are given by GPS/INS information. On the ground, additional tie points are given to avoid mismatches caused by repeating structures or areas with a low number of strong natural tie points. These points are additionally used in chapter 2.2 for the co-registration with the thermal infrared images. A bundle adjustment is done using GPS/INS exterior orientations as estimates for the unknown exterior orientations, 3D object coordinates of ground control points (GCPs) from GPS measurements in the field and the 2D image coordinates of the tie points as observations (TRIGGS et al. 1999). The interior orientation is meant to be known and introduced as

additional observations that stay constant during the recordings. Having minimized the mean squares error of the back projection of the 3D tie points to the images, a dense matching is performed using the resulting improved exterior orientations of the images to derive a grid based digital terrain model. The digital terrain model is fit to the existing digital terrain model given from the Bavarian Authorities (BLBDV).

## **2.2 Coregistration of Thermal Images and Ortho Image**

A coregistration of 2D image edges implies that the difference in the field of view and the exterior orientation of the RGB and the TIR image is small enough to ignore differences in the visibility and perspective of both images. It is also assumed that prominent edges appear in the RGB image as well as in the TIR image. The coregistration is a two-step process. In the first step, corresponding feature candidates have to be found. An affine transformation is calculated to minimize the search space for corresponding features in the TIR image and its corresponding RGB image. In a second step, the found corresponding feature points are taken to calculate the projection of the TIR image to the ortho image plane.

For the affine transformation, an edge detection based on the Sobel operator is done in both the scaled TIR and the RGB image followed by a nonmaximum-suppression. The different radiometric appearance of edges is mainly eliminated by this step. Based on the first estimation of the scale factor of the TIR image and the corresponding part of the RGB image, assuming a limited error in the exterior orientation, the coregistration is done using iterative estimation of the best transformation parameters in a similarity metric (STYNER et al. 2000). The algorithm results in an affine transformation of the TIR image to the RGB image. Based on this transformation it is assumed that the remaining differences are small enough to have a very reduced search space for corresponding point features in the TIR image and the RGB image. Following the argument, that prominent edges appear in both images, the Förstner operator (FÖRSTNER & GÜLCH 1987) is used to detect point features. The correspondences are found only based on the point positions looking for smallest distances of a homologous point candidate in the two images.

Being aware that an affine transformation is only a first estimation of the correct projection, especially in a mountainous area, the resulting homologous points of step one are now used to refine the exterior orientations of the TIR images. From step one feature points are known in the RGB images. Their 2D coordinates are projected onto the digital terrain model using the estimated exterior orientations of the RGB images from chapter 2.1. These 3D coordinates are now projected into the TIR image plane to minimize the distance of the projected RGB feature points and their corresponding TIR points in an adjustment using the 2D points as observations and the exterior orientation of the TIR image as unknowns. RANSAC (FISCHLER & BOLLES 1981) is used to remove outliers. The resulting estimated exterior orientations are used to do an ortho projection of the TIR image to add the TIR channel to the RGB ortho image.

## **2.3 Image Segmentation and Classification**

The image classification is used to extract cold areas on the meadows with an orientation along the slopes. A supervised maximum-likelihood classification is used to classify meadow and forest from the RGB channels. A segmentation is done for the classified meadow areas to detect cold areas in the TIR channel. These cold areas are supposed to be areas with high moisture, which is

an indicator for water flow. These cold segments are supposed to be thin, long structures following the slope. Morphological operators are applied to remove gaps.

## 2.4 Hydrological Modelling

The Water Balance Simulation Model WaSiM is a deterministic, mainly physically based hydrologic catchment model. It allows the simulation of the water cycle above and below the land surface based on simplified physical process descriptions. WaSiM is applicable to numerous spatial and temporal scales. The model is hence suitable for both small and very large catchments. Furthermore, WaSiM can be used for short-term and long-term simulations. As input data information on precipitation, temperature, topography, land use and soil properties are needed. Due to the extensive selection of modules, WaSiM is suitable for solving manifold hydrologic questions (SCHULLA 1997). WaSiM has been extended by a surface routing module developed and presented by WINTER (2013). This module determines the runoff concentration of the generated surface runoff according to the kinematic wave approach. The surface routing module is suitable for micro and lower meso scale applications. The flow velocity is calculated by the Manning-Strickler-equation. Gradient and surface roughness highly influence the runoff concentration in small scale applications. Due to soil compaction or exceeding of storage capacity infiltration excess is ponding on the land surface. When the depression storages are exhausted, free water starts to flow off following the slope. Then the surface routing module passes the surface runoff from cell to cell depending on the flow direction. The surface water is routed per cell until the subbasin outlet is reached. Finally the runoff is transferred to the discharge routing of the river system (Fig. 1). The surface routing module even allows the occurrence of multiple flow paths.

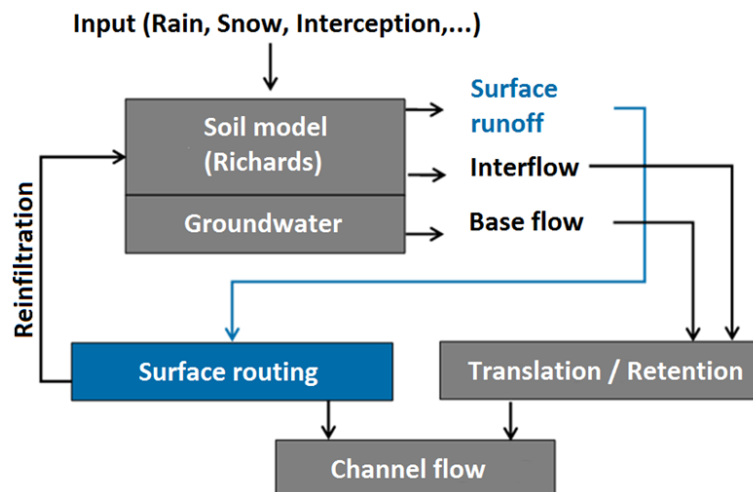


Fig. 1: Model approach: WaSiM with the implemented surface routing module (WINTER 2013)

The curvature of the area specifies whether the surface runoff is propagating in one or more flow directions. The flow velocity is computed using energy gradient, water film height and surface roughness. Subsequently, the amount of surface water flowing into each direction can be calculated. The type of cultivation determines the surface roughness and hence the flow resistance of the area. The delineation of the roughness coefficient is based on different empirical approaches.

The SR module even enables the simulation of re-infiltration and the influence of dynamic roughness and flow resistances on the flow velocity (WINTER 2013).

### 3 Experimental Setup

A flight campaign was carried out at the Sachenbach valley in the south of Bavaria (Fig. 2), where the meadow slope areas to both sides of the Sachenbach have been recorded. Figure 3a shows one exemplary flight path. For the RGB images a Sony Nex 7 was used. The Thermal infrared images were recorded using a FLIR Tau 640. Both cameras were mounted one after another onto an Ascending Technologies Falcon 8 (Fig. 3b) flying the same predefined path with both cameras.



Fig. 2: Overview of the test site. Left is the Walchensee lake. Only the meadow areas close to the valley floor are recorded. Forest areas are skipped.



Fig. 3: a) Overview of the test site. Left is the Walchensee lake. Only the meadow areas close to the valley ground are recorded. Forest areas are skipped. b) Falcon 8 with Sony Nex 7 mounted.

## 4 Results

The resulting image sequences contains image pairs in RGB (Fig. 4a) and TIR (Fig. 4b) for every recording position. Figure 3 shows one image pair of a meadow with two little brooks. The brook in the upper part of the images is clearly visible in both RGB and TIR. The one in the lower part of the images is hard to see in the RGB image but clearly visible in the TIR image. In the center of the TIR image, a few small dark structures following the slope can be seen that are moisture areas.

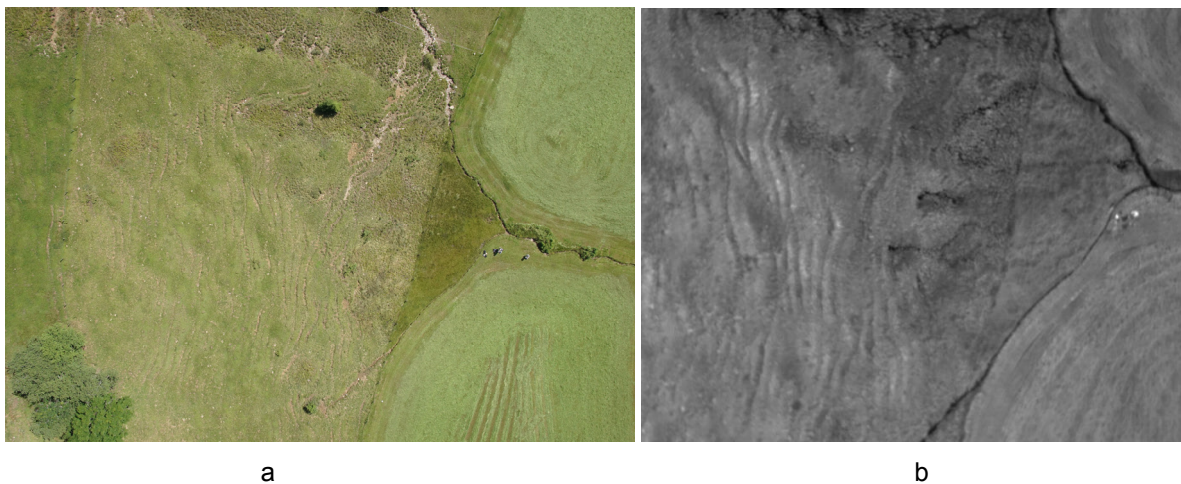


Fig. 4: Image pair a) RGB image: Only the brook in the upper part of the image is visible. b) TIR image: two brooks are visible and some additional moisture areas in the center of the image following the slope in the meadow.

### 4.1 Digital Terrain Model and Ortho Image Generation

A digital terrain model and an ortho image are derived from the bundle block of the RGB images. Figure 5 shows a 3D Reconstruction of the scene generated from the bundle block with dense matching (HIRSCHMÜLLER, 2008).

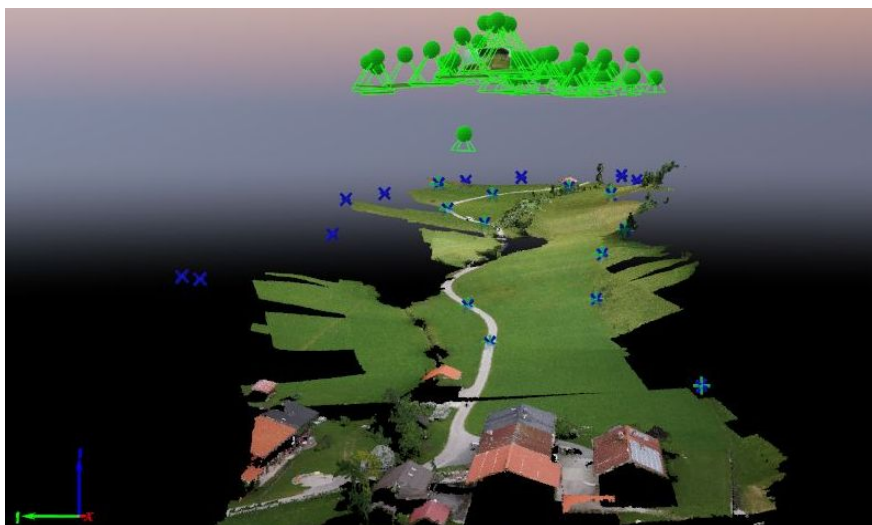


Fig. 5: 3D Reconstruction of the valley floor.

Gaps in the model are caused by trees and their different occlusions from different viewing positions. The digital terrain model is generated from the bundle block and fit to the existing thin terrain model obtained from the Bavarian Geodata Service. The resulting fused terrain model is shown in figure 6. In figure 6a the calculated dense terrain model parts derived from the bundle are shown as they fit into the given terrain model. Figure 6b shows the final fused terrain model as shaded relief model. The small squared blobs along the river are manually measured profiles of the river bed. The shaded relief model shows no artefacts along the borderlines due to the high accuracy of the generated point cloud.

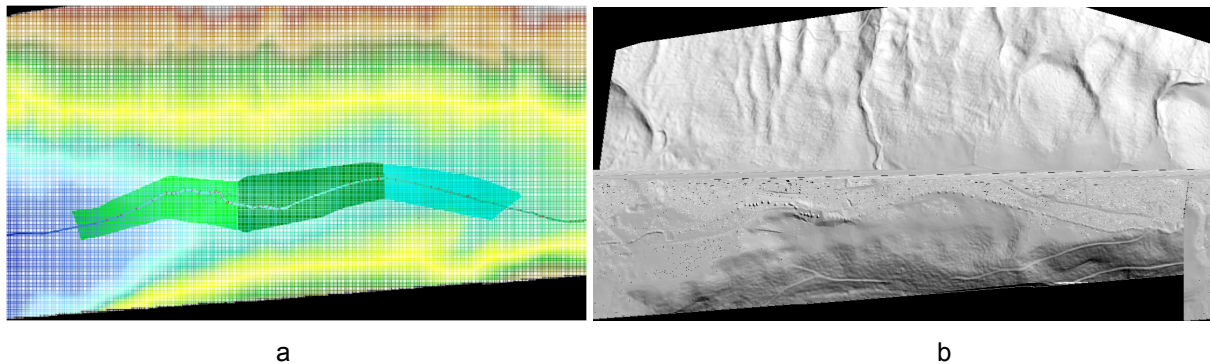


Fig. 6: Digital Terrain Model. a) Dense terrain model stripes fit into the thin terrain model. b) Fused terrain model including measured river bed profiles (small blobs).

## 4.2 Coregistration of Infrared Images and Classification

The coregistration is based on two steps. Step one is the estimation of an affine transformation to detect corresponding feature points in RGB and TIR images. A result is shown in figure 7a, where the RGB image is drawn in red and the coregistered TIR image in green. The brooks show a much higher contrast in the TIR image compared to the RGB image. River elements fit together quite well. It can be seen that in the meadow, RGB and TIR show slightly different structures. In the second step, the found corresponding feature points are used to refine the exterior orientations of the TIR images and to project the TIR images into the ortho image. Figure 7b shows the result of the second step for the image pair of figure 7a. The ortho image is drawn in RGB and overlaid with the projected TIR image in blue.

## 4.3 Hydrologically Modelling and Interpretation

The aerial image shows that the grassland is very heterogeneous. On the basis of structure and color different areas can be distinguished and severely eroded areas on the grassland can be discovered. Soil is removed by massive surface runoff and return flow. Thermal remote sensing provides information about the runoff behavior of an area. Due to the radiant temperature not only flowing waters but also water saturated soils and water outlets in the ground can be made visible. In this way, flow structures and runoff contributing areas can be visualized which are otherwise difficult or impossible to detect in the field or on aerial photographs. Therefore, areas with high surface runoff generation and surface runoff flow paths can be detected and defined as erosion prone areas (Fig. 8).

The surface runoff simulation of WaSiM with surface routing module is analyzed based on different precipitation events. Selected convective and advective precipitation events, as well as a flood event from June 2013 help evaluating the simulation of surface runoff. The surface runoff result grids provide interesting information about the runoff behavior of the basin during rain events. Convective precipitation events cause immediately high amounts of surface runoff in the Sachenbach catchment. One hour later, however, the overland flow is already significantly declined. During advective events it takes much longer until surface flow occurs on extensive areas. In return, the decline of the surface runoff is slow. WaSiM does not predict overland flow on the entire grassland area (Fig. 8). The largest part of the generated surface runoff is less than  $0.009 \text{ m}^3/\text{s}$ . Flow paths on which surface runoff accumulates to larger amounts are clearly recognizable by the darker colors. WaSiM predicts surface runoff on all plotted erosion prone areas (bordered in red). Shape and runoff amount of the two largest and most important erosion sites are remarkably well simulated. Furthermore, the lengthening or temporary formation of branches is pictured. In this context, a long temporary branch highlighted in dark purple is particular noteworthy. According to the WaSiM simulation, the highest amount of surface runoff flows off in this flow path. In summary, the surface runoff situation in the grassland area is well predicted by the surface routing model. WaSiM was even able to picture the largest erosion sites which were previously identified on aerial and thermal images.

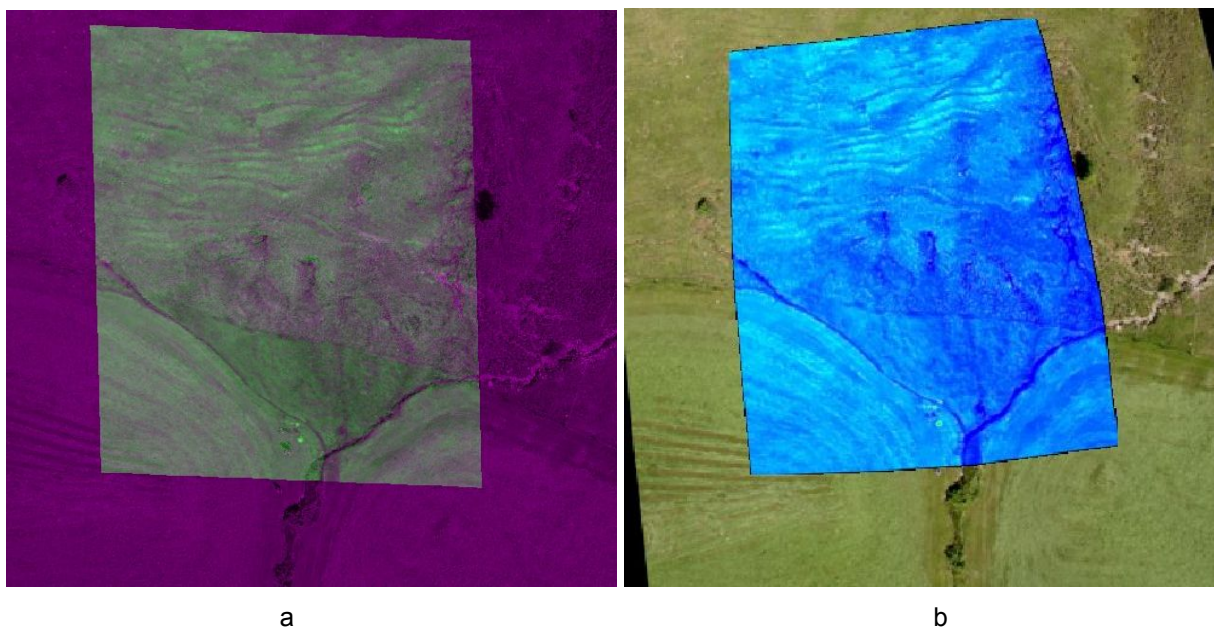


Fig. 7: RGB / TIR coregistration: a) Overlay of RGB image (red) and TIR image (green). The brooks fit together quite well. Structures on the meadow show slightly different intensities. b) TIR image (blue) projected onto the ortho image (RGB).

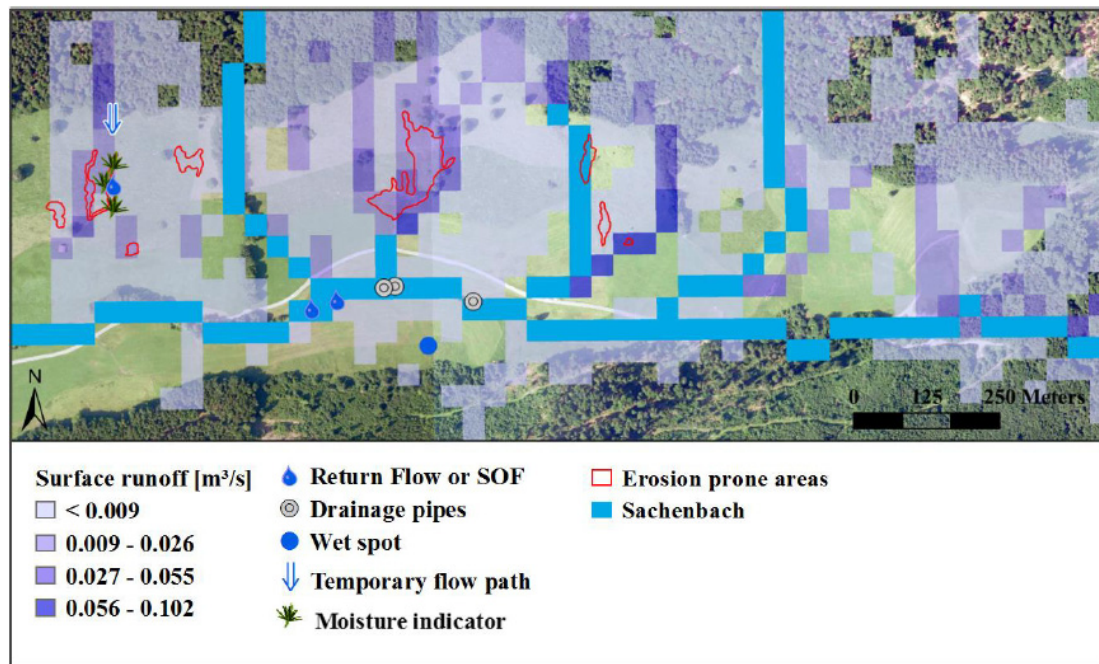


Fig. 8: Simulation of surface runoff combined with the results of the field investigation. The grassland area is shown at the time of the highest simulated surface runoff peak during the extreme weather event in June 2013 (02.06.201312:00)

## 5 Discussion and Outlook

In general, the coregistration of RGB and TIR images of landscape scenes is more complex compared to manmade scenarios with rectangular structures and straight lines. Nevertheless, a two-step process of coregistration based on feature correspondence search is possible. The number of reliable features visible in both the RGB images and the TIR images was relatively small so that the redundancy in the estimation of the exterior orientation of the TIR images is quite low. In the scenario used for this investigation the parameters of the affine transformation had to be adopted manually to the scene. This limits the methods to small bundle blocks. The flight path and recording orientation have been optimized for the RGB camera with sufficient overlap. As the TIR camera has a smaller field of view, the overlap for the TIR images was too small to directly calculate a bundle block of the TIR images, which could further improve the quality of the projection in two ways: First, the accuracy of the estimated orientation from the bundle block adjustment is better than the original recorded orientation parameters. Second, it would be possible to do a 3D reconstruction from the RGB and TIR images separately and coregister the whole image blocks using the 3D point clouds. Thermal photography enables the visualization of waterlogged areas, flow paths and sources. The application of thermal photography for hydrological issues is still unexplored but seems to be very promising. Using thermal images it could be confirmed that surface runoff occurs on the erosion sites in the Sachenbach basin.

## 6 References

- FISCHLER, M. & BOLLES, R., 1981. Random sample consensus: A paradigm for model fit-ting with applications to image analysis and automated cartography. *Communications of the ACM* **24** (6), 381-395.
- FÖRSTNER, W. & GÜLCH E., 1987. A Fast Operator for Detection and Precise Location of Distinct Points, Corners and Centers of Circular Features. *Proceedings of the ISPRS Intercommission Workshop on Fast Processing of Photogrammetric Data 1987*, 281-305.
- HIRSCHMUELLER, H., 2008. Stereo processing by semiglobal matching and mutual information. *IEEE Transactions on Pattern Analysis and Machine Intelligence* **30** (2), 328-341.
- HOEGNER, L. & STILLA, U., 2015. Building facade object detection from terrestrial thermal infrared image sequences combining different views. *ISPRS Annals of the Photogrammetry, Remote Sensing and Spatial Information Sciences* **II** (3/W4), 55-62.
- MAYER, H., BARTELTSEN, J., HIRSCHMUELLER, H. & KUHN, A., 2012. Dense 3d reconstruction from wide baseline image sets. *Outdoor and Large-Scale Real-World Scene Analysis, 15th International Workshop on Theoretical Foundations of Computer Vision*, F. Dellaert, J.-M. Frahm, M. Pollefeys, L. Leal-Taixe & B. Rosenhahn (eds), Dagstuhl Castle, Germany, June 26-July 1, 2011, **7474**, Springer, Berlin, 285-304.
- NICHOL, J. & LEE, C.M., 2004. Urban vegetation monitoring in Hong Kong using high resolution multispectral images. *International Journal of Applied Earth Observation and Geoinformation* **26** (5), 903-918.
- NICHOL, J., 2005. Remote Sensing of Urban Heat Island by Day and Night. *Photogrammetric Engineering & Remote Sensing* **71** (5), 613-621.
- SCHULLA, J., 1997: Hydrologische Modellierung von Flussgebieten zur Abschätzung der Folgen von Klimaänderungen. ETH Zürich, Dissertation.
- SCHULLA, J., 2015: Model Description WaSiM. Water balance Simulation Model. Zürich.
- STYNER, M., BRECHBUEHLER, C., SZKELY, G. & GERIG, G., 2000. Parametric estimate of intensity inhomogeneities applied to MRI. *IEEE Transactions on Medical Imaging* **19** (3), 153-165.
- TRIGGS, B., McLAUCHLAN, P., HARTLEY, R. & FITZGIBBON, A., 1999. Bundle Adjustment – A Modern Synthesis. *Proceedings of the International Workshop on Vision Algorithms ICCV '99*, Springer-Verlag, 298-372.
- WESTFELD, P., MADER, D. & MAAS, H., 2015. Generation of TIR-attributed 3D Point Clouds from UAV-based Thermal Imagery. *Photogrammetrie Fernerkundung Geoinformation* (5), 381-394.
- WINTER, F., 2013: Prozessorientierte Modellierung der Abflussbildung und -konzentration auf verschlammungsgefährdeten landwirtschaftlichen Nutzflächen. Universität der Bundeswehr, München, Dissertation.